Image Cover Sheet

CLASSIFICATION	SYSTEM NUMBER 504189
UNCLASSIFIED	

TITLE

A MATCHED-FIELD BACKPROPAGATION ALGORITHM FOR SOURCE LOCALIZATION

System Number:

Patron Number:

Requester:

Notes:

DSIS Use only:

Deliver to:

A MATCHED-FIELD BACKPROPAGATION ALGORITHM FOR SOURCE LOCALIZATION

D.J. Thomson[1] *G.R. Ebbeson*[1] *B.H. Maranda*[2]

[1]Defence Research Establishment Atlantic, Esquimalt Defence Research Detachment
CFB Esquimalt, PO Box 17000 STN FORCES, Victoria, B.C. V9A 7N2 Canada

[2]Defence Research Establishment Atlantic, PO Box 1012, Dartmouth, N.S. B2Y 3Z7 Canada

Abstract - **Model-based signal processing techniques have been developed in recent years to improve the capability of active and passive sonar systems for detecting and localizing quiet underwater targets. In a generic matched-field processor, hydrophone signals measured at the array are compared to hypothetical signals (replicas) that are calculated by a full-field acoustic model for a given target position. This matching is carried out for many potential target locations within a search region (range, depth and bearing) to form an ambiguity surface whose peak values provide the greatest likelihood that targets are present. In this paper, we evaluate a version of a matched-field processor that combines measured data with a higher-order parabolic equation algorithm to effectively backpropagate an (unnormalized) ambiguity surface outwards from the receiving array. To illustrate this PE-based method, the unconventional processor is applied to some synthetic and experimental hydrophone data received on vertical line arrays in shallow-water waveguides.**

I. INTRODUCTION

Model-based signal analysis methods such as matched-field processing have been developed and successfully applied to a wide range of problems in underwater acoustics, including the passive localization of a sound source (range, depth and bearing) and the determination of environmental parameters affecting acoustic propagation (for an overview see [1] and the references therein). Source localization by matched-field processing is carried out by correlating the fields measured on an array of hydrophones with replica fields. The replicas are predicted using a full-field propagation model with known (or assumed) input parameters chosen from a search space of candidate ranges, depths and bearings for the source position, and environmental parameters for the waveguide. The candidate source position showing the highest correlation between measured and replica fields is used to estimate the true location of the source.

For tonal signals, the basic data that is input to the matched-field processor consists of the vector $\mathbf{d}$ of complex-valued pressures obtained from an array of N hydrophones. The conventional (Bartlett) scheme compares these data to replica fields $\mathbf{r}(r,z)$ by forming, for each location (r,z) on the search grid, the scalar product

$$B_r(r,z) = |\mathbf{d}^*\mathbf{r}(r,z)|^2 \equiv \mathbf{r}^*\mathbf{C}\mathbf{r}, \qquad (1)$$

where $\mathbf{C} = \mathbf{d}\mathbf{d}^*$ is the cross-spectral matrix and * denotes conjugate transpose. Here, the vector $\mathbf{r} = \mathbf{p}/||\mathbf{p}||$ is a normalized prediction of the acoustic field $\mathbf{p}(r,z)$ on the array due to a point source located at range r and depth z.

There are a number of sophisticated propagation models suitable for computing the coherent replica fields $\mathbf{p}$ [2]. Normal mode models are particularly efficient for both matched-field [3]–[5] and matched-mode [6]–[9] localization applications in range-independent waveguides. For non-adiabatic range-dependent environments, however, models based on the parabolic equation (PE) approximation have proven to be effective [10]. Previously, we have used a PE-based procedure to carry out spectral decomposition of signals received on a vertical line array (VLA) [11]. The complex modal amplitudes determined by this method were subsequently used to successfully localize targets in some matched-field benchmark processing problems [12, 13].

The above modal decomposition and localization scheme is based on a single PE-type backpropagation calculation and is similar in spirit to another PE-based backpropagation method termed "acoustic retrogation" that was proposed and implemented several years ago for addressing the inverse source problem [14, 15]. In the present paper, we modify this original retrogation scheme by replacing the split-step Fourier PE with a higher-order PE based on the split-step Padé algorithm [16]. Moreover, to accommodate lower signal-to-noise ratios, we use a maximum likelihood method to provide an estimate of the pressure field on the VLA from a knowledge of its averaged cross-spectral matrix. The new backpropagated PE procedure is applied to signals that are available for two shallow-water scenarios: synthetic VLA data generated for the matched-field benchmark problems [17] and measured VLA data collected during the Hudson Canyon experiment [18]–[20].

II. THEORY

A. *Parabolic Approximations*

In the stratified half-space $z > 0$ (range r, depth z), the 2D one-way wave equation for the outgoing field $\psi(r,z) = p(r,z)\exp(-ik_0 r)\sqrt{r}$ is given in $r > 0$ by [21]

$$\frac{\partial \psi}{\partial r} = ik_0\left\{-1+\sqrt{1+X}\right\}\psi \qquad (2)$$

where p is the acoustic pressure and k_0 is a reference wavenumber. Here $X = N^2 - 1 + \rho k_0^{-2}\partial_z\left(\rho^{-1}\partial_z\right)$ is a

depth-dependent operator, $N = n(1 + i\alpha)$, $n = c_0/c$ is the acoustic refractive index, and c, ρ and α denote the sound speed, density and absorption, respectively. The field ψ satisfies a radiation condition as $z \to \infty$.

Higher-order PEs can be obtained from (2) by expanding the square-root operator in the Padé series [22], [23]

$$-1 + \sqrt{1+X} \approx \sum_{j=1}^{J} \frac{a_j X}{1 + b_j X} \tag{3}$$

where the coefficients a_j and b_j are given by

$$a_j = \frac{2}{2J+1} \sin^2 \frac{j\pi}{2J+1}, \quad b_j = \cos^2 \frac{j\pi}{2J+1}. \tag{4}$$

The PE obtained by substituting (3) into (2) can be solved from r to $r + \Delta r$ *serially* as a sequence of J systems of equations, where the jth system is given by

$$(1 + b_j X) \frac{\partial \psi_j}{\partial r} = ik_0 a_j X \psi_j. \tag{5}$$

The Crank-Nicolson procedure uses the approximations

$$\begin{aligned} \frac{\partial \psi_j}{\partial r} &\approx \frac{\psi(r_j, z) - \psi(r_{j-1}, z)}{\Delta r}, \\ \psi_j &\approx \frac{\psi(r_j, z) + \psi(r_{j-1}, z)}{2}, \end{aligned} \tag{6}$$

where $r_j = r + \frac{j}{J}\Delta r$ for $j = 1, \ldots, J$ combined with a standard finite-difference representation for $X\psi$ to yield J implicit tri-diagonal systems of equations.

An alternative solution procedure is based on the Padé series expansion of the PE propagator [16]. Over the range step Δr, (2) has the formal solution

$$\psi(r + \Delta r, z) = \exp\left\{ik_0 \Delta r \left(-1 + \sqrt{1+X}\right)\right\} \psi(r, z). \tag{7}$$

When $X = X(r)$, (7) can still be applied if the commutator $\partial_r X\psi - X\partial_r\psi$ is sufficiently small. Substituting (3) into the argument of the propagator in (7) and using Cayley's second-order accurate and unitary approximation of the exponential gives

$$\begin{aligned} \exp\left\{i\delta \sum_{j=1}^{J} \frac{a_j X}{1 + b_j X}\right\} &\approx \prod_{j=1}^{J} \frac{1 + c_j^+ X}{1 + c_j^- X} \\ &\equiv 1 + \sum_{j=1}^{J} \frac{a'_j X}{1 + b'_j X} \end{aligned} \tag{8}$$

where $c_j^{\pm} = b_j \pm \frac{1}{2} ik_0 \Delta r a_j$. By inspection, it is evident that $b'_j = c_j^-$ in (8). The a'_j can be found numerically by solving the linear system that results by evaluating the right-hand side at the J zeroes, $X = -(c_j^+)^{-1}$. Substituting (8) into (7) yields

$$\psi(r + \Delta r, z) = \psi(r, z) + \sum_{j=1}^{J} \psi'_j(r + \Delta r, z) \tag{9}$$

where ψ'_j satisfies

$$(1 + b'_j X)\, \psi'_j(r + \Delta r, z) = a'_j X \psi(r, z). \tag{10}$$

Because each ψ'_j depends on the same *total* field ψ on the right-hand side, the solution of (10) for $j = 1, \ldots, J$ can proceed in *parallel*.

Solutions to either (5) or (10) based on the *real* Padé coefficients in (4) often exhibit numerical fluctuations. For acoustic problems, these are due to the propagation of evanescent waves that are not effectively removed by the absorbing layer that is appended to the PE computational grid to simulate the downgoing radiation condition. The contaminating influence of these waves can be removed by replacing a_j and b_j with complex Padé coefficients which act to attenuate the evanescent waves. Suitable complex coefficients for stabilizing higher-order acoustic PEs can be obtained from a_j and b_j by rotating the branch cut of $\sqrt{1+X}$ into the lower half of the complex plane [24].

B. Backpropagated Correlation Surface

Efficient replica calculations for matched-field processing applications make use of two fundamental properties that are satisfied by one-way PE fields: reciprocity and superposition. By allowing the interchange of source and receiver positions, the former property reduces the computational effort to the generation of N replica surfaces $\mathbf{p}(r, z)$ corresponding to a point source located at each of the N hydrophone positions on the receiving array. For a VLA, the linear property allows all N replicas to be propagated at the same time. The retrogation technique initiates the solution procedure by forming the scalar product $\mathbf{d}^*\mathbf{p}(0, z)$ at the array for each point z on the PE computational grid, i.e., by weighting the vertically-extended PE source field centered at the nth sensor by the complex conjugate of the signal received on the nth hydrophone and then summing over N. This correlation measure satisfies the one-way PE and its boundary conditions, and allows the ambiguity surface to be propagated outward from the array toward the potential target locations in a single PE run.

Instead of the normalized correlation function given in (1), the backpropagation method described above yields the unnormalized correlation measure

$$B_p(r, z) = |\mathbf{d}^*\mathbf{p}(r, z)|^2. \tag{11}$$

Calculations of B_p based on (11) proceed N times faster than those for B_r based on (1) where N individual replicas must be generated and saved before the vector norm $||\mathbf{p}|| = \sqrt{\mathbf{p}^*\mathbf{p}}$ can be computed. In practice, (11) can be partially normalized by replacing $\mathbf{p}$ with $\sqrt{r}\,\mathbf{p}$.

C. Maximum Likelihood Estimator

When many observations $\mathbf{d}_l$ of the field on the array are available, an improved estimate of the cross-spectral matrix $\mathbf{C}$ can be obtained by forming the average $(1/L)\sum_{l=1}^{L} \mathbf{d}_l\mathbf{d}_l^*$. The question is how to obtain a good estimate of $\mathbf{d}$ from the averaged matrix $\mathbf{C}$. Suppose the observed data $\mathbf{d}_l$ consists of spatially-white, Gaussian noise $\mathbf{w}_l$ added to a signal of the form $\mathbf{x}_l = A\exp(i\theta_l)\mathbf{u}$. Here $\mathbf{u}$ is an N-dimensional complex vector of unit norm ($||\mathbf{u}|| = 1$), A is the amplitude and θ_l is a random phase angle. Then, it can be shown that the maximum likelihood estimate for the value $\widehat{\mathbf{d}}$ ($||\widehat{\mathbf{d}}|| = 1$) that maximizes

the sum of correlations $|\mathbf{d}_l^* \mathbf{u}|^2$ over the L snapshots is given approximately by

$$\widehat{\mathbf{d}} = \arg\max_{||\mathbf{u}||=1} \mathbf{u}^* \mathbf{C} \mathbf{u}. \tag{12}$$

The solution to (12) can be found from some standard results in matrix analysis. The maximum eigenvalue λ_1 of the N (real) eigenvalues of $\mathbf{C}$ can be expressed as the maximum of the Rayleigh quotient [25]

$$\lambda_1 = \max_{\mathbf{v} \neq 0} \frac{\mathbf{v}^* \mathbf{C} \mathbf{v}}{||\mathbf{v}||^2}. \tag{13}$$

This maximum is assumed when the (orthonormal) vector $\mathbf{v}$ is the eigenvector $\mathbf{v}_1$, i.e., $\lambda_1 = \mathbf{v}_1^* \mathbf{C} \mathbf{v}_1$. It follows that $\widehat{\mathbf{d}} = \mathbf{v}_1$ is the solution to (12). Numerically, then, we perform the eigen-decomposition of the averaged cross-spectral matrix $\mathbf{C}$, and use the eigenvector corresponding to the largest eigenvalue as the best estimate of the signal at the array hydrophones. This result is similar to one obtained recently for a problem in bearing estimation [26].

III. APPLICATIONS

In this section, the capability of the backpropagated matched-field processing method for acoustic localization is examined using both synthetic and experimental data. In each example, the receiver is a vertical line array spanning a shallow-water waveguide.

A. Synthetic Data

First, we consider the three sets of synthetic signals and noise that were generated for the general mismatch (GENLMIS) cases of the matched-field processing benchmark problems [17]. Table I shows the true values of the sound-speed, density and attenuation that were used to represent the water column (depths 0 to 104.9 m) and the bottom layers (depths greater than 104.9 m). The variation with depth between these values was taken to be linear. Because the sound-speed profile in the water is downward-refracting, there is considerable interaction of the propagating energy with the bottom. In addition, with the positive sound-speed gradient in the sediment, some of this energy will propagate within the bottom layers.

TABLE I
True Environmental Parameters for GENLMIS

Depth (m)	Sound Speed (m s^{-1})	Density (g cm^{-3})	Attenuation (dB λ^{-1})
0.0	1499.9	1.00	0.00
104.9	1478.7	1.00	0.00
104.9	1574.0	1.79	0.19
200.0	1694.0	1.79	0.19
>200	1694.0	1.79	0.19

The synthetic pressure data for the environment of Table I were generated for a 250-Hz stationary source using the KRAKEN normal mode propagation model [27]. Three different signal-to-noise ratios (SNRs) per sensor were considered: 40 dB, 10 dB and −5 dB. The simulated VLA consisted of 20 hydrophones which spanned the water column so that the first sensor was at a depth of 5 m and the spacing between sensors was 5 m. For each SNR, the pressure data on the VLA were estimated from the averaged cross-spectral matrix using (13) and then correlated with sinc-type PE source functions centered at each hydrophone depth. The ambiguity surfaces for these data were backpropagated using (11) for $J = 2$, and computational grid steps $\Delta r = 5$ m and $\Delta z = 0.5$ m. The PE grid was extended vertically to a depth of 250 m and incorporated an absorbing layer to prevent artificial reflections from the base of the grid. For localization and display purposes, the backpropagated ambiguity surfaces were interpolated from the PE grid onto a search grid having a 50-m range increment in the range interval [5 km, 10 km] and a 1-m depth increment in the depth interval [1 m, 100 m].

The localization results for the three synthetic cases are shown in Fig. 1. Each surface has been thresholded

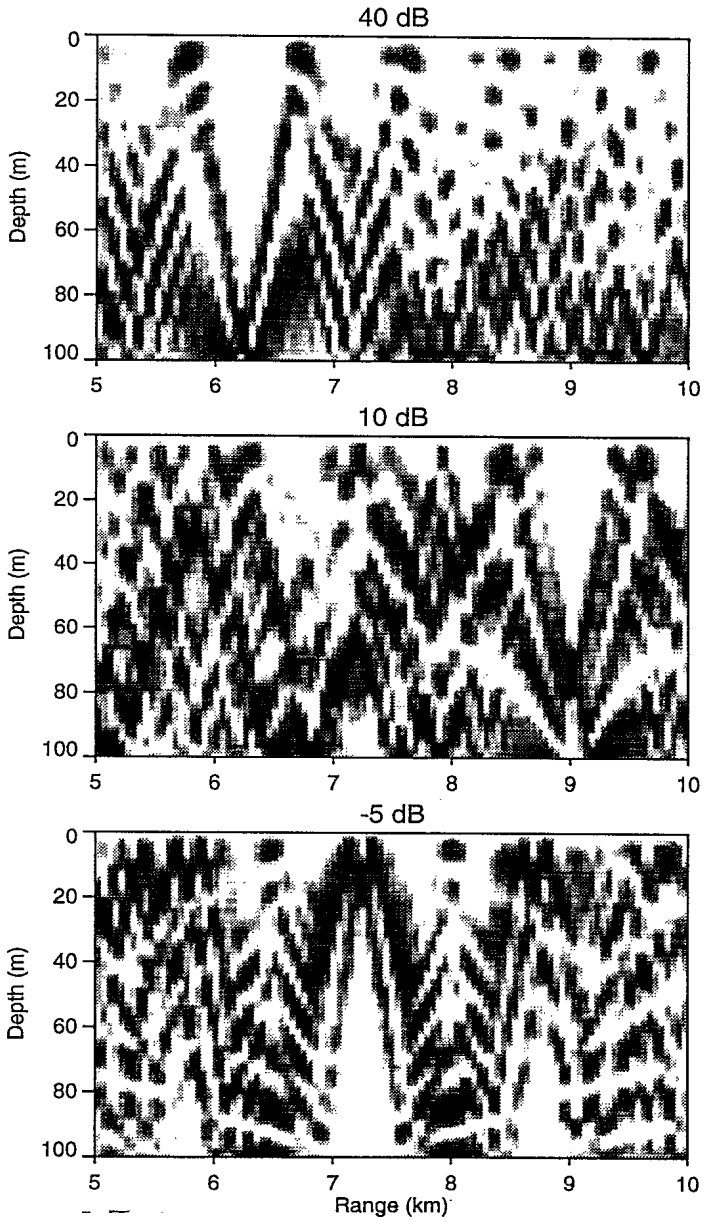

Fig. 1. Backpropagated ambiguity surfaces for the general mismatch cases of the matched-field workshop benchmark problems using the true environment.

to display only the top 15 dB. As shown in Table II, the highest peak ($\max B_p(r,z)$) found on the backpropagated ambiguity surface for each SNR corresponds to the correct location of the source.

TABLE II
GENLMIS Range and Depth Estimates

SNR (dB)	True r, z of Source (km, m)	$\max B_p\ r, z$ using Table I (km, m)	$\max B_p\ r, z$ using Table III (km, m)
40	6.2, 92	6.2, 92	5.9, 77
10	9.0, 74	9.0, 74	5.0, 97
-5	7.2, 16	7.2, 16	6.9, 16

The effect of environmental mismatch on the matched-field processor for the three SNR cases was examined by replacing the true profile of Table I with the nominal profile given in Table III. The resulting backpropagated localizations are included in Table II, where it is seen that the peaks of the ambiguity surfaces are shifted in depth and range, with the largest error occurring when the SNR is 10 dB. These results are consistent with those obtained elsewhere using the normalized processor B_r [17].

TABLE III
Nominal Environmental Parameters for GENLMIS

Depth (m)	Sound Speed (m s^{-1})	Density (g cm^{-3})	Attenuation (dB λ^{-1})
0.0	1500	1.00	0.00
102.5	1480	1.00	0.00
102.5	1600	1.75	0.35
200.0	1750	1.75	0.35
>200	1750	1.75	0.35

B. Experimental Data

Next, we present some backpropagated localization estimates for measured data obtained from the Hudson Canyon experiment that was carried out at a shallow-water location off the New Jersey coast [18]. Table IV shows the range-independent sound-speed, density and attenuation profiles that were acquired for the two (incoming and outgoing) short-range ($0-5$ km) propagation runs.

The sound speed profile in the water column (depths 0 to 73 m) is based on a mean profile taken from *in situ* XSV and CTD measurements. The geoacoustic layers (depths greater than 73 m) were deduced using a non-acoustic inversion method [28, 29]. Although previous studies of the transmission loss in this environment indicated that the upward-refracting layers between 73 m and 98 m have the most effect on propagation [18], the full profile given in Table IV was used for the backpropation calculations. The geoacoustic profile was terminated with a suitable absorbing layer. For the outgoing run considered here, four tonals were transmitted at frequencies of 50, 175, 375 and 425 Hz. The nominal depth of the towed source was 36 m. The receiving VLA consisted of 24 hydrophones spaced at 2.5-m intervals between the depths of 14.95 m and 72.45 m. Data for 20 individual ranges (10 for the outgoing track and 10 for the incoming track) that were made available from this experiment have been carefully analyzed and summarized by Michaelopoulou and Porter [19, 20] in the context of matched-field processing for acoustic localization and tracking.

TABLE IV
Environmental Parameters for Hudson Canyon

Depth (m)	Sound Speed (m s^{-1})	Density (g cm^{-3})	Attenuation (dB λ^{-1})
0	1520	1.00	0.0000
15	1520	1.00	0.0000
20	1505	1.00	0.0000
30	1492	1.00	0.0000
40	1484	1.00	0.0000
50	1485	1.00	0.0000
60	1487	1.00	0.0000
73	1487	1.00	0.0000
73–78	1560	1.86	0.0819
78–88	1610	1.96	0.1337
88–98	1740	2.09	0.2238
98–108	1830	2.17	0.1774
108–118	1760	2.09	0.0955
118–138	1710	2.03	0.1637
138–158	1740	2.05	0.2319
158–178	1910	2.18	0.1910
178–198	2010	2.24	0.1473
198–218	1980	2.21	0.1637
218–243	1940	2.17	0.1910
243–268	1850	2.10	0.1501
>268	1850	2.09	0.2729

Backpropagated results for the case where the source was 1.79 km from the array are shown in Fig. 2. They were generated using $J = 2$, $\Delta z = 0.25$ m and $\Delta r = 5$ m, and then interpolated onto a search grid with range/depth increments 50/1 m in the range interval [0 km, 5.1 km] and depth interval [1 m, 73 m]. Each of the four ambiguity surfaces that was backpropagated has been thresholded to display only the top 15 dB. The range estimates corresponding to the highest peak for each tonal surface are listed in Table V. It is observed that only 2 of the 4 peaks of $B_p(r,z)$ occur near the actual range (1.79 km) and depth (36 m) of the source for this data set.

TABLE V
Hudson Canyon Range and Depth Estimates

Frequency (Hz)	Range (km)	Depth (m)
50	0.15	66
175	1.70	33
375	1.75	34
425	2.90	32
Sum	1.70	33

Michaelopoulou and Porter have demonstrated that by combining the ambiguity surfaces for all four frequencies, either coherently or incoherently, the localization estimates for the Hudson Canyon data sets can be sufficiently enhanced to allow continuous tracking of the source for both incoming and outgoing propagation runs. In Fig. 3 we

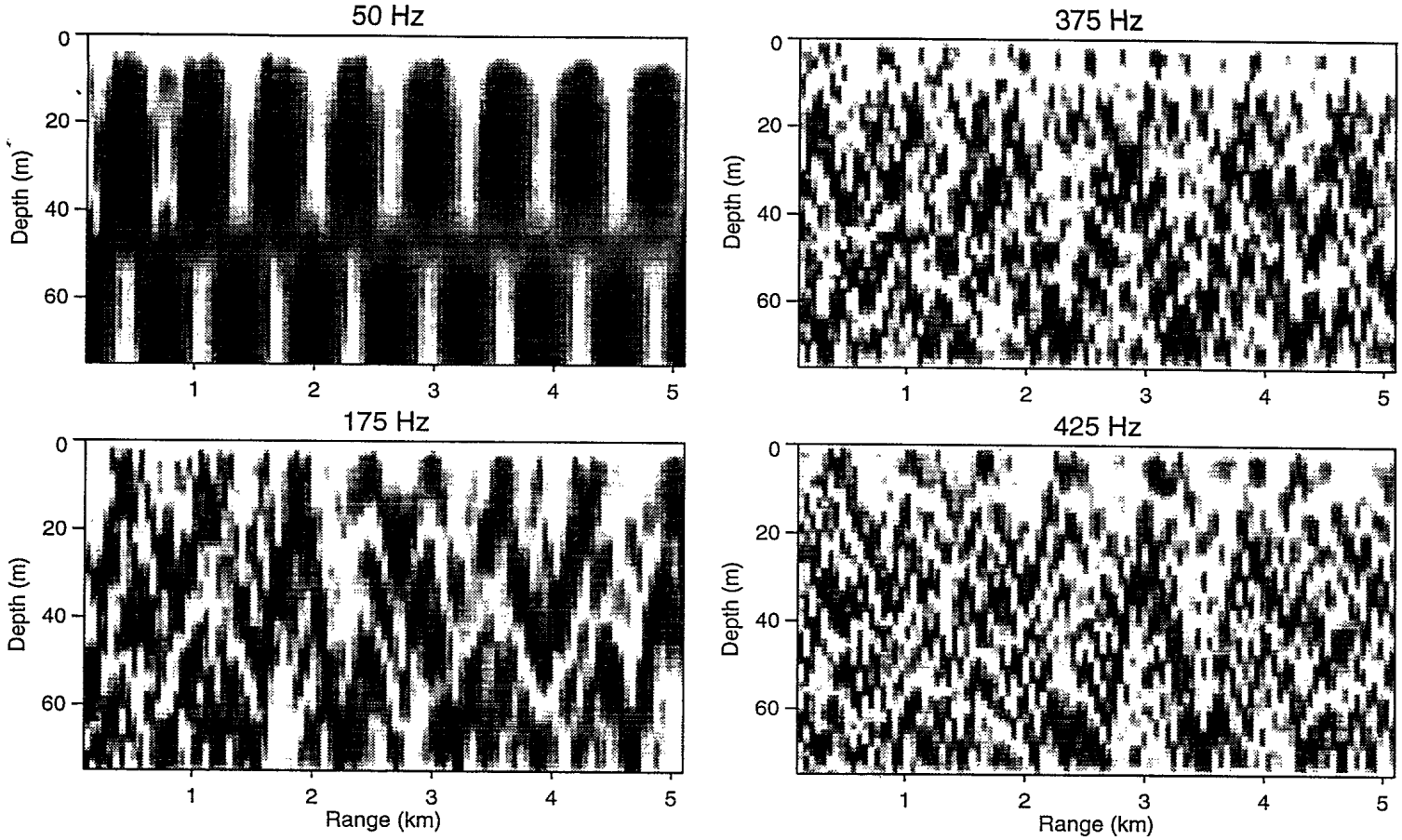

Fig. 2. Backpropagated ambiguity surfaces for the four tonals of the Hudson Canyon experiment.

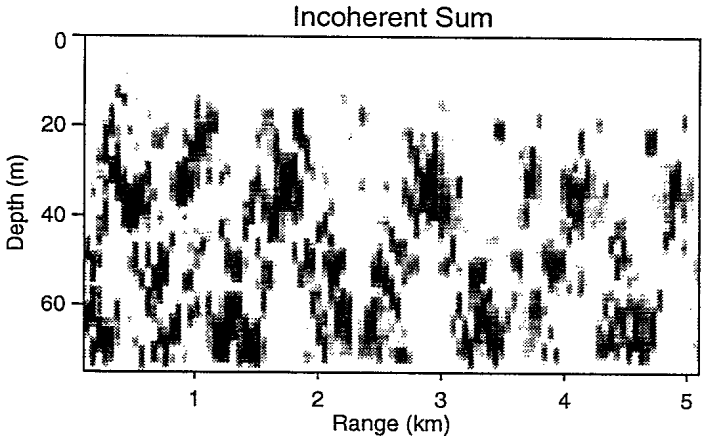

Fig. 3. Incoherent sum of the backpropagated ambiguity surfaces for the four tonals of Fig. 2.

show the result of adding the four surfaces of Fig. 2 incoherently in dB-space and then thresholding to display only the top 30 dB. The peak of this broadband ambiguity surface, which is also given in Table V, correctly locates the source for this range sample. In addition, it is seen that the peak-to-sidelobe ratio has improved.

IV. SUMMARY

In this paper, we have investigated a linear correlation processor for source localization applications that is based on a parabolic equation (PE) type backpropagation algorithm. Measured signals received by a vertical line array (VLA) due to a distant target are first correlated with vertically-extended PE starter functions centered at each sensor position. Then, using a higher-order PE model, the ambiguity surface is "retrogated" outwards from the array to span the search region of interest [14]. For an array of N hydrophones, this backpropagation method can generate an ambiguity surface N times faster than the conventional Bartlett processor, albeit with an unconventional normalization.

Two applications of the method were presented. The first involved noisy synthetic signals corresponding to the general mismatch scenario of the matched-field processing benchmark problems [17]. For this data, it was shown that given the knowledge of the true environment (i.e., no mismatch), the retrogation technique was able to successfully locate the single-tonal source for signal-to-noise ratio (SNR) levels of 40, 10 and -5 dB. The good performance of the processor at the lower SNRs was due in part to the eigenvector decomposition method that was used to provide a maximum likelihood estimate of the VLA pressure signals from the averaged cross-spectral matrix. The backpropagation technique was also carried out using a nominal environment (i.e., mismatched from the true environment). The resulting localization errors indicate that matched-field inversion techniques may be required to mitigate the effects of environmental mismatch.

The second application considered some multi-tonal data that were recorded during the Hudson Canyon experiment [18]. In this case, it was found that only 2 of the

4 tonals radiated by the towed source led to accurate localizations for the single range sample that was processed. However, following the experience of others [19], a less ambiguous estimate of source position was obtained for the linear processor by summing the individual correlation surfaces incoherently over frequency (in dB-space). Because of these encouraging results, it is planned to apply the acoustic retrogation method to the remaining 19 range/data sets for the Hudson Canyon experiment. In addition, we intend to compare these unnormalized localizations with the normalized estimates of the conventional Bartlett processor.

REFERENCES

[1] A. Tolstoy, *Matched Field Processing for Underwater Acoustics*. Singapore: World Scientific, 1993.

[2] F.B. Jensen, W.A. Kuperman, M.B. Porter and H. Schmidt, *Computational Ocean Acoustics*. New York: AIP Press, 1994.

[3] H.P. Bucker, "Use of calculated sound fields and matched-field detection to locate sound sources in shallow water," *J. Acoust. Soc. Amer.*, vol. 59, pp. 368–373, 1976.

[4] M.B. Porter, R.L. Dicus and R.G. Fizell, "Simulations of matched-field processing in a deep-water Pacific environment," *IEEE J. Oceanic Eng.*, vol. 12, pp. 173–181, 1987.

[5] J.M. Ozard, "Matched field processing in shallow water for range, depth, and bearing determination: Results of experiment and simulation," *J. Acoust. Soc. Amer.*, vol. 86, pp. 744–753, 1989.

[6] E.C. Shang, "Source depth estimation in waveguides," *J. Acoust. Soc. Amer.*, vol. 77, pp. 1413–1418, 1985.

[7] E.C. Shang, C.S. Clay and Y.Y. Wang, "Passive harmonic source ranging in wave-guides by using mode filter," *J. Acoust. Soc. Amer.*, vol. 78, pp. 172–175, 1985.

[8] T.C. Yang, "A method of range and depth estimation by modal decomposition," *J. Acoust. Soc. Amer.*, vol. 82, pp. 1736–1745, 1987.

[9] G.R. Wilson, R.A. Koch and P.J. Vidmar, "Matched mode localization," *J. Acoust. Soc. Amer.*, vol. 84, pp. 310–320, 1988.

[10] C.A. Zala and J.M. Ozard, "Matched-field processing in a range-dependent environment," *J. Acoust. Soc. Amer.*, vol. 88, pp. 1011–1019, 1990.

[11] G.R. Ebbeson, D.J. Thomson and B.H. Maranda, "Spectral decomposition of underwater sound received on a vertical line array," *IEEE Oceans Proceedings, Vol. 3, October 1-3, 1991*, pp. 1336–1343, 1991.

[12] D.J. Thomson and G.R. Ebbeson, "A propagating field approach to modal decomposition and source localization," *IEEE Oceans Proceedings, Vol. 3, October 18-21, 1993*, pp. III-91–III-96, 1993.

[13] D.J. Thomson and G.R. Ebbeson, "A PE-based approach to modal decomposition and source localization," *J. Comp. Acoust.*, vol. 2, pp. 231–250, 1994.

[14] F.D. Tappert, L. Nghiem-Phu and S.C. Daubin, "Source localization using the PE method," *J. Acoust. Soc. Amer. Suppl. 1*, vol. 78, p. S30, 1985.

[15] L. Nghiem-Phu, F.D. Tappert and S.C. Daubin, "Source localization by CW acoustic retrogation," *Workshop on Acoustic Source Localization, 20–21 November 1985, Naval Research Laboratory, Washington, DC*, Extended Abstract, 1985.

[16] M.D. Collins, "A split-step Padé solution for the parabolic equation method," *J. Acoust. Soc. Amer.*, vol. 93, pp. 1815–1825, 1993.

[17] M.B. Porter and A. Tolstoy, "The matched field processing benchmark problems," *J. Comp. Acoust.*, vol. 2, pp. 161–185, 1994.

[18] W.M. Carey, J. Doutt, R.B. Evans and L.M. Dillman, "Shallow-water sound transmission measurements on the New Jersey continental shelf," *IEEE J. Oceanic Eng.*, vol. 20, pp. 321–336, 1995.

[19] Z.-H. Michalopoulou and M.B. Porter, "Matched-field processing for broad-band source localization," *IEEE J. Oceanic Eng.*, vol. 21, pp. 384–392, 1996.

[20] Z.-H. Michalopoulou and M.B. Porter, "Source tracking in the Hudson Canyon experiment," *J. Comp. Acoust.*, vol. 4, pp. 371–373, 1996.

[21] F.D. Tappert, "The parabolic approximation method," in *Wave Propagation and Underwater Acoustics*, J.B. Keller and J.S. Papadakis Eds. New York: Springer, 1977, chap. V, pp. 224–287.

[22] A. Bamberger, B. Engquist, L. Halpern and P. Joly, "Higher order paraxial wave equation approximations in heterogeneous media," *SIAM J. Appl. Math.*, vol. 48, pp. 129–154, 1988.

[23] M.D. Collins, "Benchmark calculations for higher-order parabolic equations," *J. Acoust. Soc. Amer.*, vol. 87, pp. 1535–1538, 1990.

[24] F.A. Milinazzo, C.A. Zala and G.H. Brooke, "Rational square-root approximations for parabolic equation algorithms," *J. Acoust. Soc. Amer.*, vol. 101, pp. 760–766, 1997.

[25] R. Bellman, *Introduction to Matrix Analysis, 2nd Ed.*. New York: McGraw-Hill, 1970.

[26] D. Hertz and I. Ziskind, "Fast approximate maximum likelihood algorithm for single source localisation," *IEE Proc.-Radar, Sonar Navig.*, vol. 142, pp. 232–235, 1995.

[27] M. Porter, "The KRAKEN normal mode program," SACLANTCEN ASW Research Centre, San Bartomomeo, Italy, Memorandum SM-245, 1991.

[28] M.V. Trevorrow and T. Yamamoto, "Summary of marine sedimentary shear modulus and acoustic speed profile results using a gravity wave inversion technique," *J. Acoust. Soc. Amer.*, vol. 90, pp. 441–456, 1991.

[29] A.K. Rogers, T. Yamamoto and W. Carey, "Experimental investigation of sediment effect on acoustic wave propagation in the shallow ocean," *J. Acoust. Soc. Amer.*, vol. 93, pp. 1747–1761, 1993.

A MATCHED-FIELD BACKPROPAGATION ALGORITHM FOR SOURCE LOCALIZATION

D.J. Thomson and G.R. Ebbeson
Defence Research Establishment Atlantic, Esquimalt Defence Research Detachment,
CFB Esquimalt, PO Box 17000 STN FORCES, Victoria, B.C. V9A 7N2 Canada

B.H.Maranda
Defence Research Establishment Atlantic,
PO Box 1012, Dartmouth, N.S. B2Y 3Z7 Canada

Model-based signal processing techniques have been developed in recent years to improve the capability of active and passive sonar systems for detecting and localizing quiet underwater targets. In a generic matched-field processor, hydrophone signals measured at the array are compared to hypothetical signals (replicas) that are calculated by a full-field acoustic model for a given target position. This matching is carried out for many potential target locations within a search region (range, depth and bearing) to form an ambiguity surface whose peak values provide the greatest likelihood that targets are present. In this paper, we evaluate a version of a matched-field processor that combines measured data with a higher-order parabolic equation algorithm to effectively backpropagate an ambiguity surface outwards from the receiving array. To illustrate this PE-based method, the unconventional processor is applied to some synthetic and experimental hydrophone data received on vertical line arrays in shallow-water waveguides.

Oceans '97 Proceedings, 6-9 October 1997, Halifax, N.S.

AUTHORITY TO USE COPYRIGHT MATERIAL

Submitted herewith is a paper entitled A Matched-Field Backpropagation Algorithm for Source Localization, author(s) D.J. Thomson, G.R. Ebbeson and B.H. Maranda, for publication in your Oceans97 Proceedings.

The author(s) of this paper carried out this research on behalf of the Government of Canada, and as such the copyright in the paper belongs to the Crown, i.e. to the Canadian Government. No provision exists for the transfer of any such Crown copyright, and it would be improper for the author(s) to sign any document purporting to transfer the copyright to your organization.

However, I am authorized to provide your organization with the non-exclusive permission to use the copyright article in any way you wish, as long as its source is acknowledged. This includes your giving to others permission to translate and to reproduce in any form, providing that its source, the author(s) and the Department of National Defence are clearly indicated.

It is believed that such an authorization will provide you with all the scope for action you require, but it falls short of effecting transfer of the copyright itself.

David D...
4 July 97

for Director General,
Defence **R**esearch **E**stablishment **A**tlantic

#S04189